ARTICLE TYPE www.rsc.org/xxxxxx | XXXXXXXX

Photo-excited electroless deposition of semiconducting oxide thin films and their electrocatalytic properties

Kai Kamada* and Ayano Moriyasu

Received (in XXX, XXX) Xth XXXXXXXXX 200X, Accepted Xth XXXXXXXXX 200X
First published on the web Xth XXXXXXXXX 200X
DOI: 10.1039/b000000x

The present study demonstrates the beneficial effects of ultraviolet (UV) light irradiation on the electroless deposition of several n-type semiconducting oxide thin films from an aqueous solution. To obtain ceria (CeO_2), Ce^{3+} was oxidized to a higher valence in the presence of dissolved oxygen molecules, and was then precipitated as CeO_2 on a conductive substrate through a local cell mechanism. Irradiation of the substrate by UV light during the reaction caused the generation of photocarriers (electron and holes) in the surface oxide layer. The resultant photocarriers enabled further electrochemical reactions on the surfaces of pre-deposited CeO_2 nuclei together with the substrate surface. As a result, the deposition rate and crystallinity of the film were significantly improved by the UV light irradiation. CeO_2 thin films prepared on a Pt substrate by the proposed photoelectroless deposition method showed an electrocatalytic activity for methanol oxidation without post-annealing, in contrast to the lower activity of a film deposited in the dark. This discrepancy is discussed on the basis of film morphology and crystallinity. Furthermore, it was confirmed that electroless deposition of Sn and Pr oxide (hydroxide) was also accelerated by photoirradiation. In this paper, the photoelectroless deposition mechanism is discussed in detail, and the advantages of the proposed techniques are clarified.

Introduction

Since inorganic materials can interact with photons in various ways, a number of practical applications including energy conversion (e.g., solar cells), chemical conversion (e.g., photocatalysts), and surface morphology control (e.g., laser micromachining) have been developed. In general, processes based on photon irradiation are performed under clean, environmentally-friendly conditions. In researching the photoelectrochemistry of inorganic semiconductors,[1] much attention has been devoted to hydrogen gas production as a new energy source, and to the purification of polluted emissions using semiconductor photocatalysts. Recently, photon energy has also been employed for the development of functional inorganic materials and improvement of their properties. For example, precise particle size control of semiconductor nanoparticles by wavelength-dependent photocorrosion,[2] local electrochemical reactions by site-selective photon irradiation,[3] and photoelectrochemical etching of single-crystal or polycrystalline semiconductor electrodes[4,5] have been reported in the past decade. The utilization of photon energy for the fabrication of functional inorganic materials offers numerous advantages, such as position-selective excitation using focused light, energy selectivity by wavelength, and the promotion of homogeneous reactions, especially in the liquid phase. That is, photoelectrochemical processes can induce various reactions that are otherwise difficult to achieve.

Several research groups, ours included, have studied the effects of photoirradiation during the electrochemical deposition of thin films in solution.[6,7] In our previous paper,[8] the photoelectrochemical deposition of iron(III) oxyhydroxide thin films from an Fe^{2+} solution induced the formation of unique nanostructures. As is well known, electrochemical processes in a solution system can bring about the formation of various oxide semiconductor films on a substrate. In particular, electroless deposition is recognized as a facile technique that can lead to film growth by simple immersion of the desired substrate, without requiring an external bias. However, there are several disadvantages associated with oxide film deposition: (1) a slow diffusion-controlled reaction rate, and (2) poor crystallinity, density, and adhesion of the films without post-treatment. Moreover, film growth via electrochemical reactions is inhibited after the substrate is covered by the deposited oxide layer, which has a relatively low conductivity. It is believed that photoirradiation can effectively circumvent these problems during the electroless deposition of oxide semiconductors. Under light irradiation, the electrochemical reactions are stimulated by the generation of photocarriers (electrons and holes) in the band structure of a deposit formed in advance, which reacts with the redox species at the deposit / solution interface. Accordingly, continuous growth of oxide films can be achieved under illumination, presumably enhancing their density and crystallinity.

Among many semiconducting oxides, ceria (CeO_2, E_g ~ 3.1 eV) thin films have many attractive characteristics, such as ion-conducting,[9] sun-screening,[10] anti-corrosion,[11] and electrocatalytic properties.[12] Hence, the development of a facile solution-based method for attaining high-quality ceria thin films is an issue of great urgency. In the present paper, we demonstrate that photoirradiation during the electroless deposition of ceria thin films improves their growth rate, film

density, and adhesion by influence of the photocarriers produced in the film, and the photodeposited films have a high electrocatalytic activity for the oxidation of methanol without post-annealing. In addition, the positive effects of photoirradiation for other oxides (Pr and Sn) are demonstrated. Thus, the proposed technique is a promising method for the fabrication of semiconductor oxide thin films. The success of the present technique may explore a novel aspect with respect to utilization of photon energy.

Experimental

Photoelectroless deposition was performed in a quartz glass beaker equipped with a water jacket to control the bath temperature. The solution for CeO_2 deposition contained identical amounts of $Ce(CH_3COO)_3$ and CH_3COOH (0.05 ~ 0.20 M), and the pH of the solution was adjusted to 5.6 by the addition of a minute amount of 3 M NaOH. To perform the electroless deposition, a Pt substrate was immersed in a solution at 293 ~ 313 K for up to 24 h. During the reaction, the substrate was exposed to light from a 300 W Xe lamp. For comparison, a dark electroless deposition was also performed, in a beaker covered with aluminum foil. The open-circuit potential of the Pt substrate was monitored against a saturated Ag|AgCl reference electrode. The deposition weight was recorded using a quartz crystal microbalance (QCM) method employing a 9 MHz AT-cut quartz with Pt or C deposited on both sides. Inductively coupled plasma (ICP) analysis was carried out to determine the deposition amount of Ce after dissolving the film in a concentrated H_2SO_4 solution. The morphology and crystal structure of the as-deposited films were investigated using scanning electron microscopy (SEM), X-ray diffraction (XRD), and Raman spectroscopy. The electrocatalytic performance of the Pt substrate covered with a CeO_2 film was evaluated by anodic polarization in 5 M CH_3OH + 0.1 M K_2SO_4 solution using Ag|AgCl and Pt as the reference and counter electrodes, respectively. The potential scan was performed with a scan rate of 10 mVs^{-1}. In order to deposit Pr or Sn oxide, the Pt substrate was immersed in a 0.05 M $Pr(CH_3COO)_3$ + 0.05 M CH_3COOH (pH ~ 7 at 313 K) or 0.05 M $SnSO_4$ + 1 M H_2SO_4 solution under UV light irradiation at 293 K.

Results and discussion

Formation of transparent thin films showing interference colour was observed after electroless deposition at 313 K for 24 h in a mixed solution containing 0.05 M $Ce(CH_3COO)_3$ and 0.05 M CH_3COOH (pH = 5.6), irrespective of the light illumination. However, the color of the films was strongly dependent on the illumination, with blue films being produced in the presence of light, and yellow films in the absence of light. This discrepancy reflected either the deposition amount or the film thickness. Fig. 1a shows time evolutions of the deposition weight on Pt, as estimated from QCM measurements. In each case, the deposition weight increased monotonically with reaction time. The simple relationship between the amount deposited and the deposition time suggests a facile control over the deposition

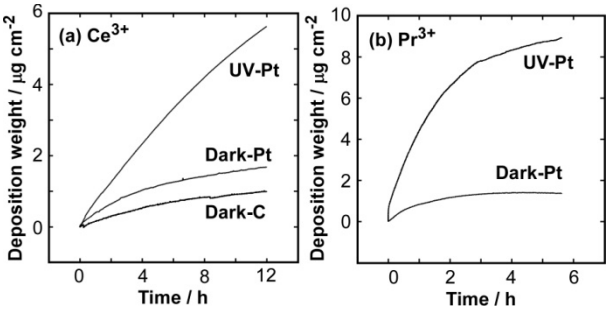

Fig. 1 Variation in the deposition weight on Pt or C substrates during electroless deposition under illumination or in the dark, as estimated from QCM measurements. (a) 0.05 M $Ce(CH_3COO)_3$ + 0.05 M CH_3COOH at pH = 5.6 and 293 K, (b) 0.05 M $Pr(CH_3COO)_3$ + 0.05 M CH_3COOH at pH = 7.1 and 293 K.

amount, at a microgram/cm^2 level, by adjusting the reaction time. In the dark state, film formation on the substrate was caused by a local cell mechanism.[13] More specifically, Ce^{3+} was oxidized by dissolved oxygen molecules through electron transfer in the Pt substrate, and was immediately transformed into a CeO_2 thin film. The Ce^{3+} in solution was coordinated with up to four acetate ligands; Ce^{3+}, $Ce(OH)^{2+}$, $Ce(Ac)_2^+$, $Ce(Ac)_2^+$, $Ce(Ac)_3$, or $Ce(Ac)_4^-$, where Ac^- indicates an acetate ion (CH_3COO^-). As reported in the previous paper,[14] the predominant species in the bath can be calculated from the ionization product of water, the dissociation constant for acetic acid, and the formation constants of the complex ions. As a result, the solution used here (0.05 M Ce^{3+} + 0.20 M total Ac^- at pH = 5.6) consisted of 7.6% Ce^{3+}, 0.0% $Ce(OH)^{2+}$, 38.2% $Ce(Ac)^{2+}$, 40.9% $Ce(Ac)_2^+$, 11.8% $Ce(Ac)_3$, and 1.4% $Ce(Ac)_4^-$. The oxidation potentials of $Ce(Ac)_x^{(3-x)+}$ (x = 1 ~ 4) were shifted to a more positive value than that of uncoordinated Ce^{3+} due to stabilization by complexing.[15] Since the potentials were located below the reduction potential of an oxygen molecule under the present conditions (e.g., $E(Ce(Ac)_2^+/CeO_2(s)) = 0.07$ V < $E(H_2O/O_2) = 0.89$ V vs. NHE, at p_{O2} = 0.2 and pH = 5.6), the dissolved oxygen molecules could oxidize the Ce^{3+} to a higher valence state. The reduction of oxygen and the oxidation of Ce^{3+} would proceed preferentially on the surface of the Pt substrate, rather than in the solution bulk, due to the high catalytic performance of the Pt substrate for oxygen reduction. As shown in Fig. 1a, the deposition rate on the C substrate, which had a low oxygen reduction activity, was slower than on the Pt substrate. In addition, the open-circuit potential of Pt shifted gradually lower during the deposition (Fig. 1S in the ESI). Because the Ce^{3+} to be oxidized was present in abundance, its concentration did not change appreciably over the entire reaction period. Taking into account the small amount of dissolved oxygen, which was responsible for the cathodic reaction, the deposition rate would be limited by the diffusion of oxygen molecules to the Pt surface. Indeed, the open circuit potential in the O_2-saturated solution was kept nearly constant during the reaction (Fig. 1S). As a result, the negative shift of the open-circuit potential probably originated from a reduction of the partial current density for the cathodic reaction. These observations support the assumption that a local cell mechanism was responsible for the electroless

deposition. Because of the lower solubility of the Ce^{IV} state than of the reduced state, Ce^{IV} would be deposited as a solid phase of CeO_2 on the Pt substrate. The consumption of protons by oxygen reduction, i.e., the generation of hydroxide ions, could increase the local pH near the Pt surface and promote the formation of CeO_2.[13]

Crystalline CeO_2 behaves as an n-type semiconductor, with a band gap of ca. 3.1 eV, which can be excited by irradiation of light with a wavelength shorter than 400 nm. Photoelectrochemical evaluation (Fig. 2S in the ESI) established that the deposited layer could act as an n-type semiconductor electrode (i.e., it generated an anodic photocurrent) without post-annealing. From the UV-vis diffuse reflectance spectrum of the film (Fig. 3S in the ESI), as-deposited by photoelectroless deposition, the film had an absorption with a shoulder at ca. 400 nm, which is consistent with the band gap energy of CeO_2 noted above.[16] Fig. 1a indicates that photoirradiation strongly enhanced the formation rate of the thin film. Since the dark reaction proceeds via a local cell mechanism, the film growth was suppressed once the substrate was covered with the deposit, which is a poor conductor. On the other hand, UV irradiation to the substrate caused band gap excitation of the pre-formed CeO_2 particles, producing electrons and holes in the conduction and valence bands, respectively. Since the oxidation potential of Ce^{3+} coordinated with acetate ions is above the upper level of the valence band, Ce^{3+} was oxidized by the holes and the CeO_2 particles continued to grow under the irradiation. Oxidation may have also proceeded via OH radicals produced as a result of the reaction between holes and water molecules. The excited electrons could reduce oxygen molecules in the solution. Since the CeO_2 nuclei acted as photoabsorbers and reaction sites for oxidation, film growth occurred without electron transport through the Pt substrate, and rapid deposition was accomplished. As shown in Fig. 1a, however, the growth curve gradually became less steep even under UV light irradiation, suggesting the consumption of dissolved oxygen and presumably the slower oxygen reduction on CeO_2 than on Pt. In summary, it was confirmed that UV light irradiation assisted Ce^{3+} oxidation and accelerated the film growth significantly. We have also confirmed that photoelectroless deposition is possible even on a non-conductive substrate after an activation treatment to deposit a Pd catalyst, which is similar to the electroless plating of metal layers.

Fig. 2 shows the influence of Ce^{3+} concentration on the electroless deposition amount. In the dark reaction, the deposition amount was slightly increased in the concentrated solution. On the other hand, the photoelectroless deposition was largely suppressed by an increase in $[Ce^{3+}]$, and the deposited amount was less than that for the dark reaction at 0.20 M. This may be explained by a photo-reductive dissolution of CeO_2.[17] Under irradiation by a photon energy significantly exceeding the band gap of CeO_2, the photogenerated electrons trapped at the CeO_2 / solution interface reduced the surface Ce^{4+}. This was followed by dissolution of the reduced species (Ce^{3+}), which have a higher solubility. As the amount of dissolved oxygen decreased, the

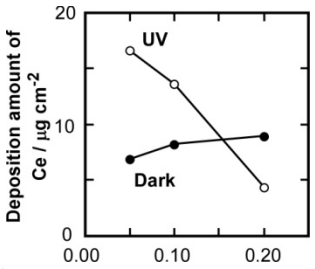

Fig. 2 Effect of Ce^{3+} concentration on the deposition amount of Ce on a Pt substrate at 313 K for 24 h, with an identical molar amount of acetic acid to that of Ce^{3+} added to the solution.

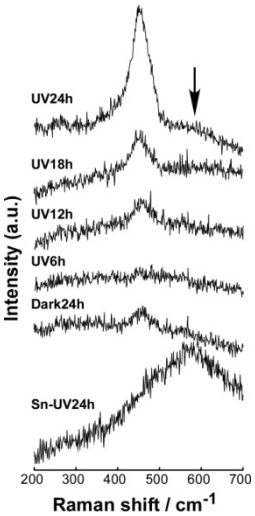

Fig. 3 Raman spectra of thin films deposited over various reaction times in 0.05 M $Ce(CH_3COO)_3$ + 0.05 M CH_3COOH at pH = 5.6 and 313 K. The spectrum of the film fabricated in 0.05 M $SnSO_4$ solution at 293 K for 24 h is also displayed (Sn-UV24h).

excited electrons were consumed by the reduction of Ce^{4+} rather than dissolved oxygen molecules. Our previous paper revealed that the presence of carboxylate anions promoted the photo-reductive dissolution of iron oxides by trapping holes produced in the valence band.[8] In the present study, under a high $[Ce^{3+}]$, i.e., a high acetate ion concentration, the effect of photo-reductive dissolution became remarkable, and decreased the deposition amount. Under our experimental conditions, the photo-assisted effect on the electroless deposition of CeO_2 thin films was most evident in dilute solution.

The crystal structure of the prepared films was studied using XRD and Raman spectroscopy. The XRD patterns of as-deposited thin films included a very weak diffraction peak attributed to the (111) plane of the fluorite crystal structure of CeO_2 (Fig. 4S in the ESI). In order to investigate the crystallinity of the film in more detail, Raman spectroscopy was performed for films prepared with various reaction times, as shown in Fig. 3. The main peak at 452 cm^{-1} observed in all spectra (excluding the "Sn-UV 24 h") corresponds to the triply-degenerate Raman active F_{2g} mode of the fluorite structure, which was detected as a symmetric breathing mode of oxygen atoms surrounding cations.[18] The peak height increased with increasing reaction time, implying the sustainable growth of a CeO_2 film during the photoelectroless

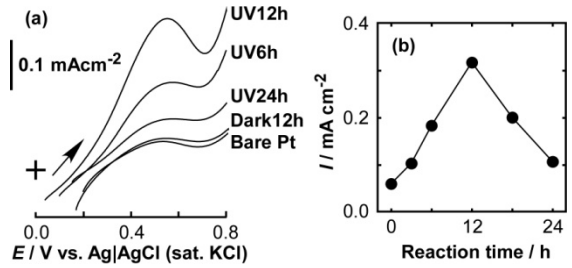

Fig. 4 (a) Anodic polarization curves (5 M CH_3OH + 0.1 M K_2SO_4 solution) of bare Pt and Pt/CeO_2 electrodes prepared by dark- or photoelectroless (UV) deposition for various reaction times. (b) Reaction time dependence of the anodic peak current density (I) corresponding to methanol oxidation at E = +0.55 V vs. Ag|AgCl (sat. KCl).

deposition. The small discrepancy of the peak wavenumber for the bulk CeO_2 crystal (464 cm^{-1}) suggests that the film was composed of tiny primary crystallites of nanometer dimensions, where the crystallite size calculated using the Raman line width (UV24h in Fig. 3) and the emprical equation given by Kosacki et al. was ca. 3 nm.[19] The small hump at the larger Raman shift (ca. 570 cm^{-1}, indicated by an arrow) corresponds to oxygen defects due to the partial reduction of Ce^{4+}.[20] In contrast, the film prepared by the dark reaction showed only a small peak, even after 24 h of reaction. These results confirm that UV irradiation during the electroless deposition is effective for the fabrication of crystalline CeO_2 films without post-treatment.

It has been reported that Pt/CeO_2/C composites show excellent electrocatalytic performance for the direct oxidation of alcohol.[12] Therefore, the electrocatalytic activity of the as-deposited CeO_2 films was evaluated by measuring their anodic polarization curves in methanol solution at 298 K. Fig. 4a shows the polarization curves of CeO_2 films on Pt, fabricated under illumination or in the dark for various reation durations. Due to the adsorption of CO on the Pt surface, the bare Pt showed no oxidation activity. On the other hand, the Pt electrodes covered with photodeposited CeO_2 (UV) showed an anodic current peak at ca. +0.55 V. These results indicate that the CeO_2 on the Pt surface reduces the overpotential for CO oxidation. Takahashi and coworkers proposed that the active oxygen species produced by interactions between oxygen vacancies in the CeO_2 surface and water molecules promotes the oxidation of CO.[21] Consequently, the CeO_2 thin film containing oxygen vacancies, which were detected by Raman spectroscopy, contributed to the anodic oxidation current observed in Fig. 4a. On the contrary, the polarization curve of the film prepared in the dark was nearly identical to that of the bare Pt substrate, indicating a lower activity for the anodic oxidation of methanol due to a small depostion amount (Fig. 1a). Fig. 4b plots the anodic peak current at +0.55 V as a function of the photoelectroless deposition time. In the figure, the peak current rises with increasing reaction time and reaches a maximum at 12 h. These results are consistent with the observed film morphology. Fig. 5 shows SEM images of films formed under various conditions. The film prepared in the dark for 24 h (Fig. 5a) had no distinct particles. The observed small pores may have provided diffusion paths for oxygen molecules to be reduced at the Pt surface.

Photoelectroless

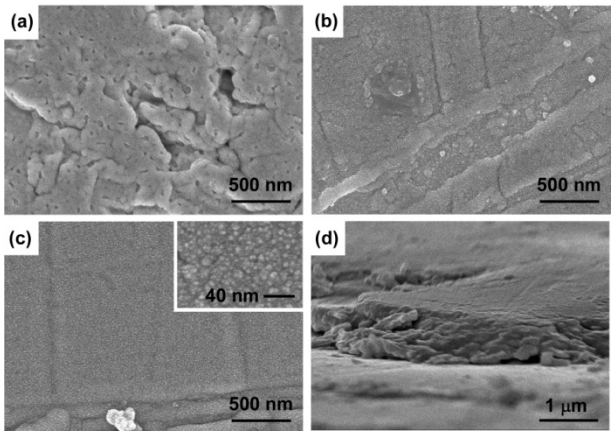

Fig. 5 Surface SEM images of as-deposited thin films deposited under dark conditions for 24 h (a) and under UV illumination for 12 h (b) or 24 h (c). Cross-sectional image of (c) is also displayed in (d).

deposition for 24 h (Fig. 5c and d) resulted in the formation of a relatively smooth film (thickness < 1 μm) composed of small particles with diameters of a few nm (inset in Fig. 5c). This supports the idea that the film growth proceeds homogeneously on the surface of the CeO_2 particles, rather than at the Pt surface under the UV light irradiation. A relatively bumpy surface that may have reflected the surface roughness of the Pt substrate was observed in the film prepared for 12 h (Fig. 5b). In contrast, a smooth and dense microstructure was observed after 24 h of reaction (Fig. 5c), as noted previously. The oxidation of methanol and oxidative removal of CO adsorbed on the Pt surface should occur at the three-phase boundary between Pt, CeO_2, and the methanol solution. For deposition times over 12 h, the thick, dense CeO_2 film could act as a barrier against methanol penetration toward the three-phase boundary. Consequently, even though the anodic current was increased by CeO_2 deposition at the initial stage, the electrocatalytic activity of the film diminished with increasing reaction time after 12 h. On the other hand, due to poor crystallinity or a lower deposition amount, films fabricated by the dark reaction had no electrocatalytic activity. Therefore, CeO_2 films deposited by photoelectroless deposition were capable of electrocatalytic methanol oxidation without any post-treatment. The activity depended upon film morphology and crystallinity. A dense, thick film formed after a longer deposition time, as shown in Fig. 5c, and appeared to act as an efficient barrier layer against the penetration of electrolytes. Hence, the dense CeO_2 thin films prepared here may be adopted as anti-corrosion layers to protect structural materials, because CeO_2 is harmless and has a self-healing ability similar to conventional chromate barrier coatings.[22]

The rare-earth element Pr^{3+} can also be oxidized to a higher valence, and then transformed into an insoluble oxide. Therefore, the photoelectroless deposition of Pr^{IV} oxide was carried out in a $Pr(CH_3COO)_3$ solution with an acetic acid additive. According to the literature,[23] Pr^{3+} can be oxidized to the Pr^{IV} state at pH > 6, so the pH of the solution was adjusted

to ca. 7. Fig. 1b shows the variation of the deposition weight during photo- and dark-electroless deposition. UV light irradiation clearly accelerated the film formation. XRD analysis of the obtained films revealed the presence of a crystalline Pr_6O_{11} phase. We also investigated the possibility of photoelectroless deposition of Sn^{IV} oxide, which also behaves as an n-type semiconductor with a band gap of 3.5 eV and has many important applications, such as sensors and transparent electrodes.[24] In this case, an acidic $SnSO_4$ solution was employed in order to stabilize Sn^{2+} in the solution. The influence of UV irradiation on film formation was stronger than for Ce or Pr. While no deposition occurred in the dark, UV light irradiation caused the deposition of a blue, transparent film. The Raman spectrum of the film (Sn-UV24h in Fig. 3) included a broad band assigned to Sn^{IV} hydrous oxide.[25] However, deposition of the film was possible not only on a Pt substrate but also on other non-conductive substrates, such as quartz glass and alumina ceramics, suggesting that the formation mechanism of the film in $SnSO_4$ solution was dissimilar to the photoelectroless deposition of CeO_2. Recently, it has been reported that UV light irradiation of a Sn^{2+} solution induces the production of mesoporous SnO_2 particles at the solution - air interface.[26] In this case, the photo-assisted disproportionation of Sn^{2+} produces Sn^0 and Sn^{4+}. The Sn^{4+} is hydrolyzed to produce insoluble H_2SnO_3, which decomposes into SnO_2 during drying. On the other hand, the reduced species (Sn^0) is oxidized to SnO_2 at the air - solution interface. Consequently, thin film deposition seems to occur through a photochemical reaction rather than a local cell mechanism. Therefore, photoirradiation during electroless deposition may be effective for other kinds of semiconductor oxide thin films.

Conclusions

The present study investigated the effect of UV light irradiation on the electroless deposition of several n-type semiconductor thin films (Ce, Pr, and Sn oxide). For CeO_2, the formation mechanism of oxide thin films was explained by a local cell mechanism involving electron transfer at the Pt substrate. Specifically, dissolved oxygen acted as an oxidizer of the metal ions, and the oxidized metal species were deposited as an insoluble oxide film on the substrate. UV light irradiation enhanced the deposition rate and the density of the film, indicating that the photocarriers, which were produced in pre-formed oxide nuclei by the UV light excitation, photocatalytically promoted the reduction of dissolved oxygen and the oxidation of metal ions. The deposition rate was also affected by the concentration of reactant; that is, a high concentration resulted in a decrease of the deposition amount due to photoreductive dissolution. The obtained Pt/CeO_2 thin films demonstrated varying activities for the electrocatalytic oxidation of methanol. This activity depended heavily on the porosity and crystallinity of the films, which could be controlled by the deposition time. On the other hand, it was confirmed that Pr_6O_{11} and Sn^{IV} hydrous oxide thin films were also formed by UV irradiation of Pr^{3+} and Sn^{2+} solutions, respectively, and the deposition of Sn^{IV} hydrous oxide proceeded through a photochemical reaction initiated by the disproportionation of Sn^{2+}. In addition to Ce, Pr, and Sn, there are many other semiconductor oxides that can be formed by the anodic oxidation of metal ions of lower valence (TiO_2, etc.). The same photo-assisted effect is expected for the electroless deposition of these oxides on various conducting and non-conducting substrates. Moreover, the photochemical technique enables on-site fabrication, because the reaction is enhanced only within the irradiated area. The present technique should be useful in the fabrication of many different kinds of metal oxide and complex oxide thin films.

Acknowledgements

The present study was partly supported by Special Coordination Funds for Promoting Science and Technology, MEXT, Japan: "The Nagasaki University Strategy for Fostering Young Scientists".

Notes and references

[a] *Department of Materials Science and Engineering, Faculty of Engineering, Nagasaki University, Nagasaki 852-8521, Japan. Fax: 81 95 8192667; Tel: 81 95 8192667; E-mail: kkamada@nagasaki-u.ac.jp*

† Electronic Supplementary Information (ESI) available: Figures showing change of open circuit potential during electroless deposition of CeO_2, photoelectrochemical property, UV-Vis reflectance spectra and XRD patterns of CeO_2 films. See DOI: 10.1039/b000000x/

1 K. Bernhard and A.J. Bard, *J. Am. Chem. Soc.*, 1978, **100**, 4317-4318; S. Sato, A. Sobczynski, J.M. White, A.J. Bard, A. Campion, M.A. Fox, T.E. Mallouk and S. E.; Webber, *J. Photochem. Photobiol. A*, 1989, **50**, 283-290.

2 T. Torimoto, J. Paz Reyes, K. Iwasaki, B. Pal, T. Shibayama, K. Sugawara, H. Takahashi and B. Ohtani, *J. Am. Chem. Soc.*, 2003, **125**, 316-317; T. Torimoto, H. Kontani, Y. Shibutani, S. Kuwabata, T. Sakata, H. Mori and H. Yoneyama, *J. Phys. Chem. B*, 2001, **105**, 6838-6845.

3 R.C. Hayward, D.A. Saville and I.A. Aksay, *Nature*, 2000, **404**, 56-59.

4 S. Nakanishi, T. Tanaka, Y. Saji, E. Tsuji, S. Fukushima, K. Fukami, T. Nagai, R. Nakamura, A. Imanishi and Y. Nakato, *J. Phys. Chem. C*, 2007, **111**, 3934-3937; A. Tsujiko, T. Kisumi, Y. Magari, K. Murakoshi and Y. Nakato, *J. Phys. Chem. B*, 2000, **104**, 4873-4879.

5 H. Masuda, K. Kanezawa, M. Nakao, A. Yokoo, T. Tamamura, T. Sugiura, H. Minoura and K. Nishio, *Adv. Mater.*, 2003, **15**, 159-161; T. Oekermann, T. Yoshida, J. Nakazawa, S. Yasuno, T. Sugiura and H. Minoura, *Electrochim. Acta*, 2007, **52**, 4325-4333.

6 C. Scheck, Y.-K. Liu, P. Evans, R. Schad, A. Bowers, G. Zangari, J.R. Williams and T.F. Issacs-Smith, *Phys. Rev. B* **2004**, *69*, 35334-35341; J.A. Switzer, *J. Electrochem. Soc.*, 1986, **133**, 722-728; Y. Matsumoto, M. Noguchi and T. Matsunaga, *J. Phys. Chem. B*, 1999, **103**, 7190-7194; M. Takahashi, M. Todorobaru, K. Wakita and K. Uosaki, *Appl. Phys. Lett.*, 2002, **80**, 2117-2119; Y. Sugimoto and L.M. Peter, *J. Electroanal. Chem.*, 1995, **386**, 183-188; K. Murase, M. Matsui, M. Miyake, T. Hirato and Y. Awakura, *J. Electrochem. Soc.*, 2003, **150**, C44-C51.

7 K. Kamada, K. Higashikawa, M. Inada, N. Enomoto and J. Hojo, *J. Phys. Chem. C*, 2007, **111**, 14508-14513.

8 K. Kamada, T. Hyodo and Y. Shimizu, *J. Phys. Chem. C*, 2010, **114**, 3707-3711.

9 Z. Shao and S.M. Haile, *Nature*, 2004, **431**, 170-173.

10 T. Masui, M. Yamamoto, T. Sakata, H. Mori and G.-y. Adachi, *J. Mater. Chem.*, 2000, **10**, 353-357; T. Masui, H. Hirai, R. Hamada, N. Imanaka, G.-y. Adachi, T. Sakata and H. Mori, *J. Mater. Chem.*, 2003, **13**, 622-627; M. Yamashita, K. Kameyama, S. Yabe, S. Yoshida, Y. Fujishiro, T. Kawai and T. Sato, *J. Mater. Sci.*, 2002, **37**, 683-687.

11 H. Ardelean, I. Frateur and P. Marcus, *Corr. Sci.*, 2008, **50**, 1907-1918; Y. Hamlaoui, F. Pedraza and L. Tifouti, *Corr. Sci.*, 2008, **50**, 2182-2188.

12 C. Xu and P.K. Shen, *Chem. Comm.*, 2004, 2238-2239; C. Xu, P.K. Shen and Y. Liu, *J. Power. Sources*, 2007, **164**, 527-531; C.L. Campos, C. Roldán, M. Aponte, Y. Ishikawa and C.R. Cabrera, *J. Electroanal. Chem.*, 2005, **581**, 206-215.

13 M.A. Arenas and J.J. de Damborenea, *Electrochim. Acta*, 2003, **48**, 3693-3698.

14 E.A. Kulp, S.J. Limmer, E.W. Bohannan and J.A. Switzer, *Solid State Ionics*, 2007, **178**, 749-757.

15 A.Q. Wang and T.D. Golden, *J. Electrochem. Soc.*, 2003, **150**, C616-C620; T.D. Golden and A.Q. Wang, *J. Electrochem. Soc.*, 2003, **150**, C621-C624.

16 X.-H. Lu, X. Huang, S.-L. Xie, D.-Z. Zheng, Z.-Q. Liu, C.-L. Liang and Y.-X. Tong, *Langmuir*, 2010, **26**, 7569-7573; G.-R. Li, D.-L. Qu, L. Aruraut and Y.-X. Tong, *J. Phys. Chem. C*, 2009, **113**, 1235-1241.

17 M.I. Litter and M.A. Blesa, *J. Colloid Interface Sci.*, 1988, **125**, 679-687; M. Grätzel, J. Kiwi, C.L. Morrison, R.S. Davidson and A.C.C. Tseung, *J. Chem. Soc. Faraday Trans.*, 1985, **81**, 1883-1890

18 M.-F. Luo, Z.-L. Yan, L.-Y. Jin and M. He, *J. Phys. Chem. B*, 2006, **110**, 13068-13071; S. Kanakaraju, S. Mohan and A.K. Sood, *Thin Solid Films*, 1997, **305**, 191.

19 F. Zhang, S.-W. Chan, J.E. Spanier, E. Apak, Q. Jin, R.D. Robinson and I.P. Herman, *Appl. Phys. Lett.* **2002**, *80*, 127-129; I. Kosacki, T. Suzuki, H.U. Anderson and P. Colomban, *Solid State Ionics* **2002**, *149*, 99-105.

20 H. Takamura and N. Takahashi, *Solid State Ionics*, 2010, **181**, 100-103.

21 M. Takahashi, T. Mori, F. Ye, A. Vinu, H. Kobayashi and J. Drennan, *J. Am. Ceram. Soc.*, 2007, **90**, 1291-1294; M. Takahashi, T. Mori, A. Vinu, H. Kobayashi, J. Drennan and D.-R. Ou, *J. Mater. Res.*, 2006, **21**, 2314-2322.

22 M.A. Arenas and J.J. de Damborenea, *Surf. Coatings Tech.*, 2004, **187**, 320-325; M.G.S. Ferreira, R.G. Duarte, M.F. Montemor and A.M.P. Simões, *Electrochim. Acta*, 2004, **49**, 2927-2935; W.G. Fahrenholtz, M.J. O'Keefe, H. Zhou and J.T. Grant, *Surf. Coatings Tech.*, 2002, **155**, 208-213; K. Aramaki, *Corros. Sci.*, 2004, **46**, 1565-1579.

23 M. Pourbaix, in *Atlas of Electrochemical Equilibria in Aqueous Solutions*; National Association of Corrosion Engineers: Houston, Texas, 1974, pp. 193.

24 S.-L. Chou, J.-Z. Wang, H.-K. Liu and S.-X. Dou, *Electrochem. Comm.*, 2009, **11**, 242-246; S.T. Chang, I.C. Leu and M.H. Hon, *J. Cryst. Growth*, 2004, **273**, 195-202.

25 M. Ristić, M. Ivanda, S. Popović and S. Musić, *J. Non-Cryst. Solids*, 2002, **303**, 270-280.

26 H. Wang, F. Sun, Y. Zhang, L. Li, H. Chen, Q. Wu and J.C. Yu, *J. Mater. Chem.*, 2010, **20**, 5641-5645; M. Ichimura, K. Shibayama and K. Masui, *Thin Solid Films*, 2004, **466**, 34-36.